Wiley
Journal of Chemistry
Volume 2025, Article ID 1236702, 12 pages
https://doi.org/10.1155/joch/1236702

WILEY

Research Article

Antibacterial Activity and Optimal Eco-Friendly Synthesis of Silver Nanoparticles Derived From an *Aloe vacillans Forsskål* Extract

Ahmed N. Al-Hakimi,[1] **Yasmin M. S. Jamil**,[2] **Hussein M. A. Al-Maydama**,[2] **Ghadeer Y. Al-Mahwiti**,[2] **Ashwaq Qasem**,[3] **Hassan M. Ibrahim**,[4] **Basem Al-Akhali**,[4] **and Sayed M. Saleh**[1]

[1]*Department of Chemistry, College of Science, Qassim University, Buraidah 51452, Saudi Arabia*
[2]*Department of Chemistry, Faculty of Science, Sana'a University, Sana'a 12231, Yemen*
[3]*Department of Chemistry, Faculty of Science, Ibb University, Ibb, Yemen*
[4]*Department of Biological Science, Faculty of Science, Sana'a University, Sana'a 12231, Yemen*

Correspondence should be addressed to Yasmin M. S. Jamil; y.jamil@su.edu.ye

Received 22 May 2024; Revised 27 September 2025; Accepted 23 October 2025

Academic Editor: Sohini Basu Roy

Copyright © 2025 Ahmed N. Al-Hakimi et al. Journal of Chemistry published by John Wiley & Sons Ltd. This is an open access article under the terms of the Creative Commons Attribution License, which permits use, distribution and reproduction in any medium, provided the original work is properly cited.

The process of producing metal nanoparticles via plant extract synthesis is not only straightforward but also economical, expeditious, and environmentally sustainable. It is consequently implemented in an extensive range of disciplines. In the process of producing silver nanoparticles (AgNPs), an extensive variety of plant extracts was employed. The production of silver nanoparticles was conducted using an environmentally sustainable method in this investigation. A reducing and stabilizing agent was derived from the aqueous extract of the *Aloe vacillans Forsskål* plant. In order to ascertain the ideal conditions for silver nanoparticle synthesis, an examination of the effects of a number of process parameters was required. The reactant volume ratio, pH values, and temperature were among these parameters. An aqueous solution of $AgNO_3$ was incorporated into an aqueous extract of the *A. vacillans* plant under optimal conditions to obtain crystalline and stable silver nanoparticles. The green-produced AgNPs were investigated and characterized through the utilization of a variety of techniques (UV-Vis spectrophotometer, FTIR, XRD, SEM, EDX, and XPS). It was demonstrated by means of the SEM technique that AgNPs possess a tetrahedral morphology. The X-ray diffraction analysis identified the dimensions of crystalline AgNPs as 19.59 nm. Antibacterial properties of optimally synthesized AgNPs are significant and efficacious against a wide range of bacterial species, as determined by dosing experiments. In this work, the antioxidant activity studies for these synthesized AgNPs revealed a moderate effect for the DPPH free radicals at various concentrations.

Keywords: *Aloe vacillans*; antibacterial activity; antioxidant activity; green synthesis; nanoparticles; silver

1. Introduction

Nanotechnology is a fascinating field that explores the creation and control of nanomaterials, which are tiny particles ranging in size from one nanometer to one hundred nanometers [1, 2]. These particles have several potential uses in diverse industries, including the surrounding environment [3], plants [4], cosmetics [5], foodstuffs [6], optics [4, 7], medicinal [8], catalysis [9], and others. Metal nanoparticles (MNPs) produced using ecologically sustainable methods are becoming more popular due to their energy efficiency, safety, cost-effectiveness, and environmentally benign characteristics [10, 11]. Metal nanoparticles (MNPs) have distinct characteristics in shape, surface chemistry, physical properties [12], and optical qualities when compared to their larger counterparts [13, 14].

Nanomaterial researchers have focused specifically on AgNPs, among other MNPs, due to their distinctive attributes and versatility. The intrinsic aspects of manufacturing

include the manufacture of various gadgets, optical sensors, electrical conductors, catalysts, and drug delivery [15]. Furthermore, AgNPs [16, 17] are used in the production of lotions, sunscreen goods, and ointments. The AgNPs have also shown substantial antibacterial efficacy [18, 19]. NPs are commonly synthesized by three primary methods: chemical, physical, and green synthesis [20, 21]. Physical nanomaterial synthesis procedures require elevated temperatures, high-pressure conditions, and expensive equipment. The chemical production of AgNPs involves the use of toxic solvents, costly metal salts, stabilizers, and reductants, which pose significant dangers to the environment and human health [22, 23]. The limits imposed by physicochemical techniques hinder the practicality of nanoparticle fabrication.

Reducing waste, using recyclable materials, applying procedures that lower hazards, and reducing energy are the primary goals of green chemistry [24]. The use of green chemistry fulfills the need for organic compounds, such as glycosides, alkaloids, tannins, phenols, terpenoids, flavonoids, or coumarin, to cover the surfaces of the nanoparticles. These chemicals serve as both active linkers and surfactants [25, 26]. Green chemistry and nanobiotechnology have the potential to create new and useful products that improve human activities while also reducing the use of dangerous reagents in the manufacturing of nanoparticles. Green chemistry plays a significant role since it has contributed to the development of novel techniques for synthesizing gold and silver nanoparticles from plant extracts, which show exceptional qualities, including antibacterial capability [27].

For the production of NPs, a variety of techniques have been employed, such as chemical reduction, electrochemical, photochemical, and physical techniques, such as physical vapor condensation [28]. Presently, scientists have identified the exact green routes, that is, naturally occurring sources and the products derived from them, which can be utilized to synthesize nanoparticles [29]. The green synthesis method involves the use of biological resources, such as plants and microbes [19]. Plant extracts are used to produce nanoparticles by simply mixing the extract with a metal salt solution at different rates depending on the parameters [30].

Table 1 summarizes some of the studies on the fabrication of nanoparticles using plant extracts. The *Aloe* genus is a monocotyledon plant with more than 600 taxa. *Aloe vacillans Forsskål* is a native variety of *Aloe* and a common species in the southwestern section of the Arabian Peninsula, located to the southwest of the peninsula [51]. The range of *A. vacillans Forsskål* encompasses the Asir Province Mountains in Saudi Arabia, as well as much of the Yemeni Mountains. It grows mostly alone, rarely suckering to form small colonies, and has small, rosulate, glaucous leaves that are ascending or erect with brown teeth on the margins and red or yellow perianths [51, 52]. Furthermore, a number of researchers have created nanoparticles using the environmentally friendly *Aloe Vera* species methodology. Prior research on *A. vacillans* mostly examined its phytochemical composition and its antibacterial properties.

Our previous research [1] used the *Aloe fleurentinorum* plant to produce AgNPs utilizing a green approach under different synthesis circumstances. The optimal values were $V/V = 1/1$, pH = 8, temperature = 60°C, and an average particle size of 26.9 nm. Furthermore, the results of the biological studies indicated that the *Escherichia coli* bacteria had the greatest effect. However, as part of the thesis study, we recently employed *A. vacillans* to discuss the comparisons. The current study aims to investigate the biological and physical properties of silver nanoparticles manufactured by an environmentally friendly method employing an aqueous extract of the Yemeni-grown *A. vacillans* plant.

2. Experimental

2.1. Materials. Silver nitrate (MICROTRADE, UK), diluted ammonia, ethanol, methanol, DPPH (SIGMA), deionized water (DIW) from a college of science, and the *A. vacillans* plant were fetched from Sana'a (Yemen).

2.2. Characterization and Investigation Techniques. Nanoparticle optimum syntheses were checked using an ultraviolet and visible double-beam spectrophotometer—SPECTROD200 (analytik Jena)—with range (300–700), and reduction and capping agent for the nanoparticles were observed by Fourier transform infrared (FTIR) spectrometer with a wavenumber ranging from 4000 to 400 cm^{-1}. The AgNPs structure and crystalline properties were studied using XD-2 (Shimadzu ED-720) powder X-ray diffractometer at a voltage of 36 kV, a current of 20 mA using CuK (α) radiation in the range of $5 < 2\theta < 75$, and a wavelength of 1.54056 Å at 1° min^{-1} scanning rate. The morphology of the AgNPs was observed by QUANTA FEC 250 scanning electron microscopy (SEM). The X-ray photoelectron spectroscopy (XPS) analyses were applied using a K-ALPHA (Thermo Fisher Scientific, Waltham, MA, USA) with monochromatic X-ray K-alpha radiation, −10 to 1350 eV, spot size 400 µm, at pressure 10^{-9} mbar, with full-spectrum pass energy 200 eV, and narrow-spectrum 50 eV.

2.3. Methods

2.3.1. The Preparation of A. vacillans Extract. The leaves of *A. vacillans* (AVL) were collected by Dr. Hassan Ibrahim, Sana'a, Yemen, during the wintertime of 2022. The AVL plant was washed multiple times with distilled water. Then, it was dried at 25°C for a few days; the dried plant was converted into powder. Next, 5 g of AVL powdered leaves was added to 100 mL DIE and stirred at 60°C for 30 min using a magnetic stirrer; then, the extract was left to cool and finally filtered and kept in a refrigerator for the next use.

2.3.2. The Silver Nanoparticle (AgNPs) Green Synthesis. A silver nitrate solution was prepared with a 10-mM concentration, and the $AgNO_3$ solution was added to the AVL aqueous extract under variant conditions, such as the reactant ratio, pH value, and temperature, to obtain the desired nanoparticles at the optimum conditions.

2.3.2.1. The Reactant Ratio Optimization. Four solutions (Y_1, Y_2, Y_3, and Y_4) were prepared with ratios 1/1, 1/2, 1/3, and 1/4 by adding different volumes of the 0.01-M prepared silver nitrate to a constant volume of the aqueous extract at

Table 1: Some of the studies on the fabrication of nanoparticles using plant extracts.

Plant name	Plant part	AgNPs size (nm)	Morphology	App.	Ref.
Aloe vacillans	Leaves	19.6	Tetrahedral	Antibacterial + Antioxidant	Current study
Aloe fleurentinorum	Leaves	26.9	Tetrahedral	Antibacterial	[1]
Allium cepa	Peels	8.44	Spherical	Antioxidant + Antipathogenic + Anticholinesterase	[31]
Callistemon lanceolatus	Leaves	41.93	Face-centered cubic	Antimicrobial + Antioxidant + Photocatalytic	[32]
Croton macrostachyus	Leaf + park	8.9–10.8	Rod + Spherical	Antibacterial	[33]
Haloxylon ammodendron	Leaves	10.97	Spherical	Antibacterial + Antifungal + Anticancer	[34]
Acer oblongifolium	Leaves	3–5	Rod-like	Antiproliferative + Antibacterial	[35]
Ligustrum vulgare berries	Fruit	20–70	Spherical	Antibacterial	[36]
Aloe Vera	Leaves	14.0	Spherical	—	[37]
		36.61	Spherical	Antibacterial	[38]
		49–82	Spherical	Antimicrobial	[39]
		—	—dsb	Antimicrobial	[40]
Tectona grandis	Seeds	10–30	Oval-spherical	Antimicrobial	[41]
Selaginella myosurus	Leaves	33.7	Spherical	Anti-inflammatory	[42]
Spondias mombin	Leaves	65–90	Spherical	Antibacterial	[43]
Taxus baccata	Needle	75.1	Spherical	Anticancer	[44]
Curcuma longa	Tuber	6.30	Spherical	—	[45]
Ocimum sanctum (Tulsi)	Leaves	17	Spherical	Antibacterial	[46]
Azadirachta indica	Seeds	34.43	spherical	Antidiabetic	[47]
Vetiveria zizanioides	leaves	—	—	Antioxidant	[48]
Euphorbia rigida	leaves	75	spherical	Antimicrobial	[49]
Lallemantia royleana	leaves	34.5	spherical	Biopharmaceutical + Catalytic applications.	[50]

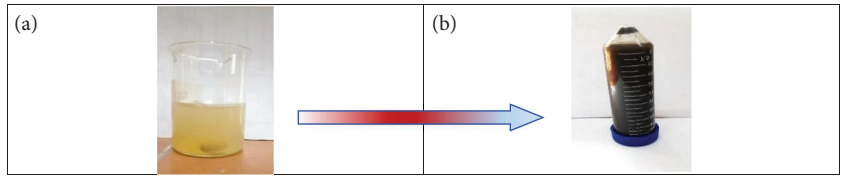


Figure 1: Visual observation of green synthesis AgNPs using *Aloe vacillans* extract: (a) before synthesis and (b) after synthesis.

pH = 7 using diluted ammonia solution and letting them stir at lab temperature for 120 min.

2.3.2.2. The pH Value Optimization. By selecting the optimum reactants ratio and altering the pH medium using aqueous ammonia solution to obtain pH = 6, 7, 8, 9, which were labeled as Y_5, Y_6, Y_7, and Y_8, respectively.

2.3.2.3. Optimization of the Reaction Temperature. Y_9, Y_{10}, Y_{11}, and Y_{12} solutions were prepared at different reaction temperatures, 25°C, 45°C, 60°C, and 80°C, respectively, after selecting the optimum previous conditions.

2.3.3. Antibacterial Activity of AgNPs. Biological properties for the green-synthesized silver nanoparticles by AVL extract were studied using the technique of disc diffusion [53, 54]. The AgNPs' antibacterial activities were determined against two pathogenic types of bacteria, Gram-negative bacteria (*Salmonella typhi* and *E. coli*) and Gram-positive bacteria (*Staphylococcus aureus* and *Bacillus subtilis*). In this test, the bacterial cells were inoculated on Petri dishes, and then we made holes in the bacterial dishes. After that the holes filled with different concentrations of synthesized AgNPs (100%, 75%, 50%, 25%) were prepared from AgNPs solution at the optimum condition's synthesis, which labeled Y_{100}, Y_{75}, Y_{50}, and Y_{25}, respectively, and the positive control uses the antibiotic (Gentamycin, 2 mg/mL), and it has been mentioned in our previous work [55]. Afterward, at 37°C, the dishes were incubated for 24 h. Then, the inhibition zones around the AgNPs samples were measured in mm.

2.3.4. Antioxidant Activity of AgNPs Using the DPPH Method. The DPPH free radical scavenging method was used to evaluate the antioxidant activity for AgNPs [32, 56]. In this approach, a 3-mM DPPH solution was prepared and then incubated in the dark for 60 min. Different concentrations of silver nanoparticles in methanol (1500, 1000, 500, 250, and 125 µg/mL) were prepared. Subsequently, 1 mL of the freshly prepared DPPH solution was added to 1 mL of different concentrations of AgNPs separately and mixed well. The mixture was incubated in the dark for 30 min. Then, the change of the color was measured by a UV-VIS spectrophotometer at 517 nm. And 1 mL of the freshly prepared DPPH solution was added to 1 mL of methanol as a control solution.

3. Results and Discussion

3.1. UV-Vis Spectroscopic Measurement. For determination and optimization, the formation of the green-synthesized silver nanoparticles, the ultraviolet-visible spectral was used, which observed the color change at different conditions [34]. The visual color transformation from pale yellow to dark brown confirmed the formation of silver nanoparticles, as shown in Figure 1.

3.1.1. The Effect of Reactant Ratio. The UV-Vis absorption spectrum of the extract in Figure 2, compared with the spectra of the green-synthesized silver nanoparticles, verified the AgNPs' formation at a constant volume of AVL and different volumes of $AgNO_3$ (0.01 M) from Y_1 to Y_4. The absorbance peaks indicate that increasing $AgNO_3$ volume from 10 mL to 40 mL causes an increase in AgNPs' formation, then a decrease, so the optimal volume ratio determined for the green-synthesized AgNPs as Y_2, which had the reactants' 1:2 volume ratio, had the highest absorption peak.

3.1.2. The Effect of pH Values. The effect of pH on the AgNPs formation by changing the pH values from pH = 6 to pH = 9. The UV-Vis absorbance peak decreased to the lowest value, then increased, and the highest absorbance peak's shift occurred at a wavelength 438 nm. These prove the formation of AgNPs. So, the optimal pH value for the green-synthesized AgNPs is Y_5 at pH = 6, as shown in Figure 3.

3.1.3. The Effect of Temperature. UV-Vis spectra of green-synthesized AgNPs at various temperatures are shown in Figure 4. It shows that the absorbance peaks decreased and shifted to a red wavelength. The maximum absorbance peak at the blue-shifted wavelength for the sample Y_9 was at a temperature of 25°C. That indicates the optimal reaction temperature at the lap temperature value.

The UV-Vis spectra of silver nanoparticles synthesized using *A. vacillans* extract showed surface plasmon resonance (SPR) peaks in the range of 430–450 nm, confirming the formation of AgNPs. A representative sharp peak at 438 nm in Figure 3 indicates the collective oscillation of conduction electrons. Variations in the SPR position among samples (Y_5–Y_{12}) may be attributed to differences in particle size, shape, and degree of aggregation, which are known to influence the λ max of AgNPs.

3.1.4. Determination of the Band Gap Energy. When surface plasmon electrons absorb light at a resonant frequency, a part of this energy is transferred into heat, and part of this energy is radiated as PL, and recombination occurs between electrons of the sp band with a hole in the d band [46]. The bandgap energy (E_g) as calculated from Tauc's plotting (Figure 5) for the synthesized AgNPs was at the optimized condition.

The optical bandgap of the biosynthesized AgNPs was estimated as 2.2 eV using Tauc's plot. While metallic silver

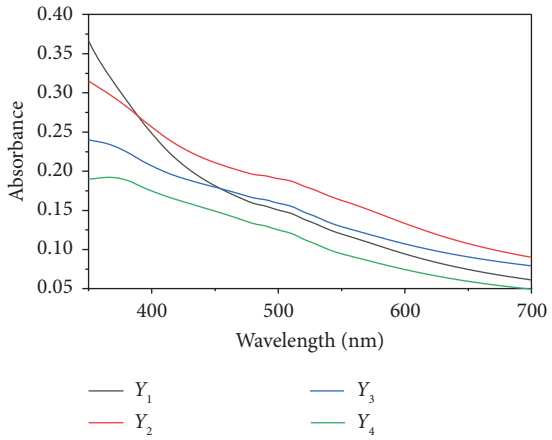


Figure 2: The UV-Vis absorption spectra of AgNPs at different reactant ratios.

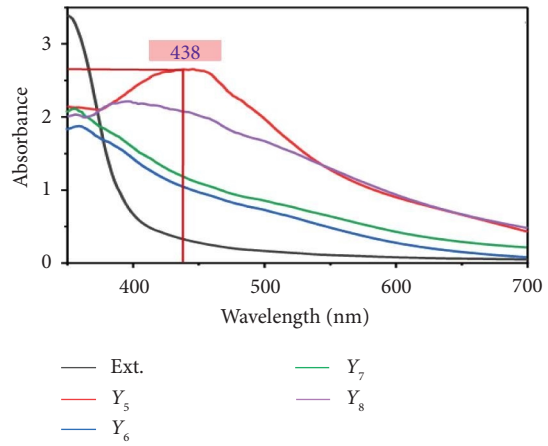


Figure 3: The UV-Vis absorption spectra of AgNPs at different pH values.

does not possess a true bandgap, XRD confirmed the co-existence of metallic Ag and silver oxide phases. The apparent E_g value can therefore be attributed to the semiconducting contribution of nanoscale silver oxide Ag_2O, which is known to exhibit E_g values between 1.2 and 2.5 eV. This hybrid composition explains the observed optical behavior and is consistent with previously reported Ag/Ag_2O nanostructures.

3.2. FTIR Spectroscopic Measurement. FTIR is shown in Figure 6 for the *A. vacillans* leaf extract and the synthesized AgNPs. It shows a broad stretching vibration band of OH for AVL extract at ~3400 cm^{-1}, suggesting phenolic groups, which decay in intensity in AgNPs IR spectra. That indicates that this bond is used in the reduction process for silver ions to AgNPs. Peaks near 1600 cm^{-1} indicate C=O or aromatic C=C. These functional groups likely reduce Ag^+ and stabilize the NPs.

3.3. XRD Studies. Figure 7 shows the X-ray diffraction patterns of dried Ag and Ag_2O nanoparticles' crystallinity phases synthesized at 25 C using AVL extract at pH 6. By

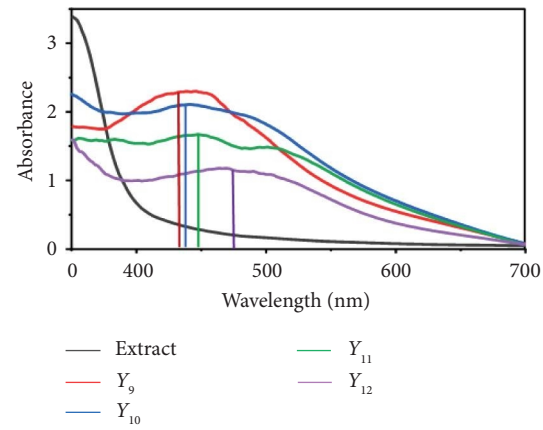


Figure 4: The UV-Vis absorption spectra of AgNPs at different temperatures.

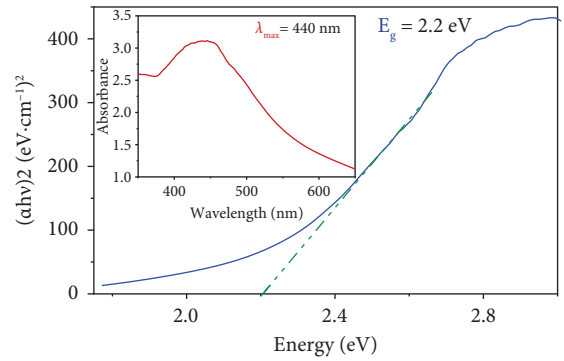


Figure 5: The bandgap energy of green-synthesized AgNPs.

comparing this position of peaks with standard XRD cards, the peaks at 38.51 , 44.65 , 64.81 , and 77.76 correspond to the planes (111), (200), (220), and (311) for Ag (JCPDS No.87-0719). Furthermore, the peaks at 32.66 and 46.65 correspond to the planes (111) and (200) for Ag_2O nanoparticles (JCPDS No.76–1393). These silver/silver oxide nanoparticles have a face-centered shape. The values of green-synthesized size, interplanar d-spacing, and microstrain are shown in Table 2 and were calculated using the following equations.

$$D = \frac{K\lambda}{(\beta \cos \theta)}, \quad (1)$$

$$d = \frac{\lambda}{2 \sin \theta}, \quad (2)$$

$$\text{strain} = \frac{\beta}{4 \tan \theta}, \quad (3)$$

where D is the average particle size, K is a constant (0.94), λ is the wavelength of the X-ray (1.5406 Å), β is the full width at half maximum (FWHM) of the peak (rad), d is the plane spacing, and θ is the position of the diffraction peak in radians [57].

Additionally, the lattice parameters for the synthesized Ag/Ag_2O-NPs, the volume, dislocation density, porosity, and determined density from X-ray data were calculated using equations (4)–(8), respectively, which are displayed in Table 3.

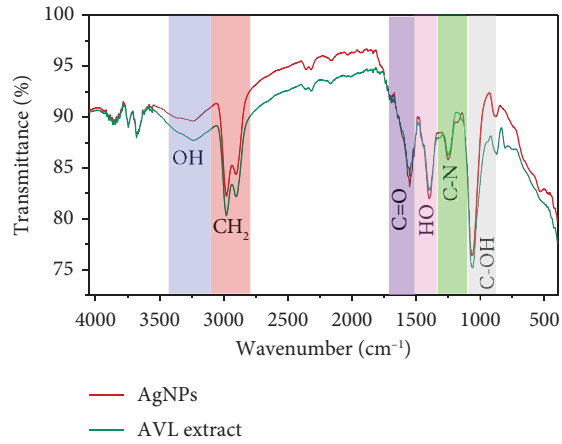


Figure 6: The FTIR absorption spectra of AVL extract and green-synthesized AgNPs.

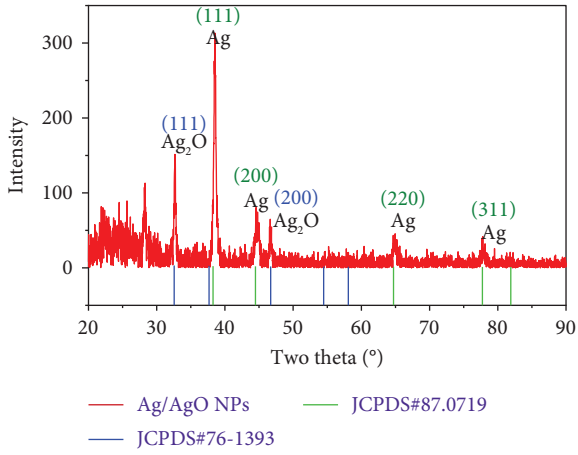


Figure 7: The pattern of X-ray diffraction.

Table 2: Interplanar d-spacing, crystalline sizes, and microstrain of AgNPs.

NPs	2θ (°)	β (°)	d (Å)	D (nm)	(ε)
Ag	38.51	0.35	2.336	25.1020	0.00053
	44.65	0.88	2.028	10.1889	0.00157
	64.81	0.77	1.437	12.7583	0.00213
	77.76	0.89	1.227	11.9714	0.00313
Ag_2O	32.66	0.24	2.74	36.0116	0.00030
	46.65	0.42	1.946	21.5055	0.00079
Average				**19.59**	**0.00141**

Note: The bold values indicate the mean values obtained from the independent measurements.

$$a = d \times \sqrt{\left(h^2 + k^2 + l^2\right)}, \tag{4}$$

$$V = a^3, \tag{5}$$

$$\delta = \frac{1}{D^2}, \tag{6}$$

$$\text{Porosity \% } (P) = \left[1 - \frac{\rho}{\rho_x}\right] \times 100, \tag{7}$$

where (h, k, l) are the Miller indices, d is the plane spacing determined through Bragg's equation (2). The $(a = b = c)$ is the lattice parameters for the synthesized AgNPs, which have a face-centered cubic (FCC) crystallinity, δ is the dislocation density [58], V is the volume, p is porosity, ρ_x is the theoretical density, and ρ is the determined density from X-ray data using the following equation.

$$\rho = \frac{ZM}{NV}, \tag{8}$$

where Z is the number of chemical units in one crystal unit cell = 4, M is the molecular weight (107.87 g/mole), N is Avogadro's number, and V is the volume.

3.4. Energy Spectrum Component Analysis. By utilizing energy-dispersive X-ray (EDX) spectrometry, the elements were analyzed. The EDX images of AgNPs, which are presented in Figure 8, exhibit distinct peaks that correspond to elements present in the plant, including some metals, such as Ag, K, Na, and other atoms, including O, N, and C. This substantiates the application of the *A. vacillans* plant as a reducing agent in the fabrication process of silver nanoparticles. The elemental analysis of the silver nanoparticles that were synthesized using XRD spectrometry is presented in Table 4.

The relatively low silver content observed in the EDX analysis (4.22%, Mass%, and 6.58% Atom%, in Table 4) is acknowledged and can be attributed primarily to the significant presence of organic matrix derived from the *A. vacillans* plant extract. This is further supported by the high percentages of carbon (14.04% Norm%) and oxygen (23.31% Norm%) detected, consistent with the biomolecules responsible for capping and stabilizing the biosynthesized silver nanoparticles. While EDX provides elemental composition rather than a direct measure of reduction efficiency, the clear silver peaks in the EDX spectrum (Figure 8) confirm the successful formation and presence of silver nanoparticles. Despite current experimental limitations precluding further complementary elemental quantification analyses, the presented EDX data effectively illustrate the elemental composition of the synthesized material, demonstrating the successful integration of silver within the biogenic matrix. The EDX analysis revealed a silver content of 4.22% by mass. This relatively low value is attributed to the organic biomolecules from *A. vacillans* extract, as indicated by the high carbon and oxygen signals. It should be noted that EDX is mainly qualitative, while more accurate quantification of Ag loading (e.g., ICP-MS) will be addressed in future work.

3.5. SEM. The SEM pictures of the silver nanoparticles (AgNPs) revealed their synthesis in the form of tetrahedral particles, as seen in Figure 9(a). *A. vacillans*, a plant species, has great potential in the manufacture of silver nanoparticles. Utilizing advanced SEM methods with improved resolution enabled the detection of silver nanoparticles that had a tetrahedral morphology, as seen in Figure 9(b). The application of *A. vacillans* plant extract in the production of

Table 3: Lattice parameters, X-ray density, dislocation density, and porosity of AgNPs.

NPs	2θ (°)	*h*	*k*	*l*	*d* (Å)	*a* (Å)	*V* (Å^3)	*δ* (nm^{-2})	*ρ* (g/cm^3)	ρ_x (g/cm^3)	Porosity%
Ag	38.51	1	1	1	2.336	4.046	66.237	0.0016	10.817	10.617	1.88
	44.65	2	0	0	2.028	4.056	66.726	0.0096	10.738		1.14
	64.81	2	2	0	1.437	4.064	67.144	0.0061	10.671		0.51
	77.76	3	1	1	1.227	4.069	67.394	0.0069	10.632		0.13
Ag_2O	32.66	1	1	1	2.74	4.746	106.889	0.0008	6.703	7.134	6.038
	46.65	2	1	1	1.946	4.767	108.307	0.0022	6.616		7.268
Average					1.86	4.291	80.445	0.0045	8.667		1.54804

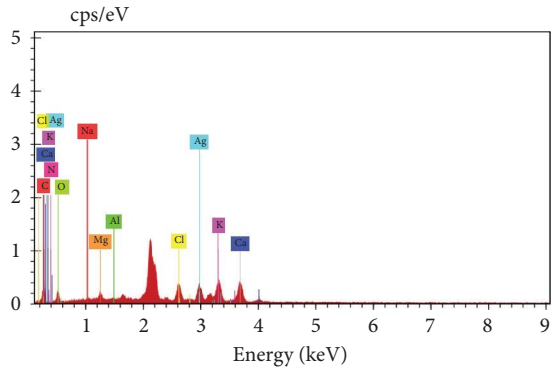


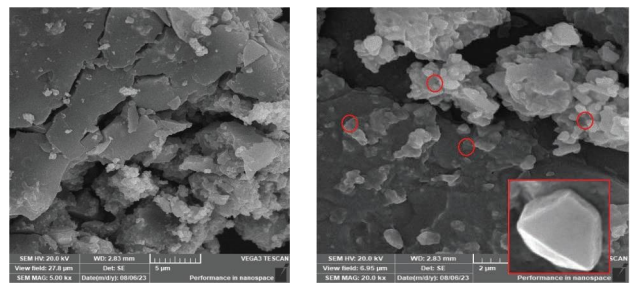
Figure 8: EDX patterns of AgNPs synthesized based on the *A. vacillans* plant.

Table 4: Elemental analysis of the as-synthesized AgNPs.

Element	At. no.	Netto	Mass %	Mass norm %	Atom %	Abs. error % (1 sigma)	Rel. error (%) (1 sigma)
Oxygen	8	435	6.11	23.31	36.38	1.32	21.24
Calcium	20	1622	4.88	18.95	10.52	0.31	4.25
Silver	47	1582	4.22	18.33	6.58	0.32	4.27
Carbon	6	482	3.65	14.04	25.85	0.72	22.58
Potassium	19	1542	2.85	12.4	8.11	0.11	3.99
Chlorine	17	1592	1.75	7.46	6.12	0.11	4.58
Magnesium	12	265	0.45	2.37	1.95	0.05	11.88
Nitrogen	7	42	0.45	2.35	3.76	0.41	72.31
Sodium	11	135	0.15	0.66	0.61	0.06	25.62
Aluminum	13	46	0.02	0.12	0.12	0.01	11.2

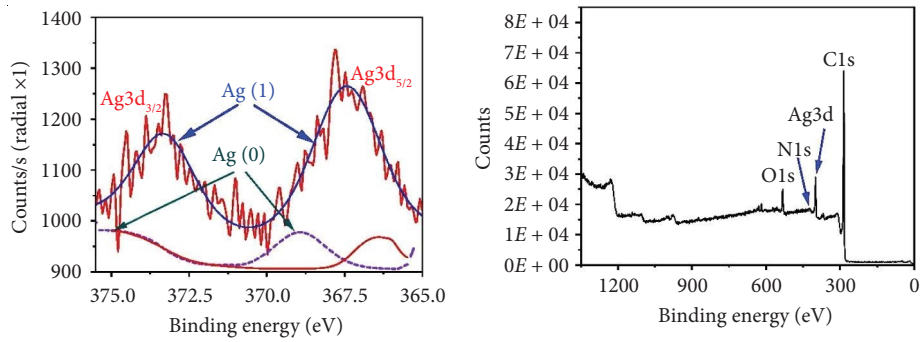
silver nanoparticles led to the effective creation of silver nanostructures, as confirmed by the SEM picture. SEM analysis revealed tetrahedral-like particles, providing valuable qualitative insight into surface morphology. However, particle size distribution histograms are more reliably constructed from TEM images, which were not available in the present study.

3.6. XPS Measurement. Deconvolution confirms the coexistence of two silver species: a dominating Ag (0) component and a small Ag (I) component, essential for establishing the chemical composition of the produced nanoparticles, as confirmed by the high-resolution Ag 3-d XPS spectrum. The ideal reduced state and primary active core for the silver nanoparticles made from the *A. vacillans* extract is metallic, zero-valent silver Ag (0), as seen by the Ag 3-d 5/2 peak centered at around 367.2 eV. The smaller part, which shows a positive binding energy shift of around 1.0 eV (peak centered at 368.2 eV), is probably formed by oxidized silver Ag (I), which is likely to have a thin layer of silver oxide (Ag_2O) on its surface. Since the Ag (0) surface is quickly oxidized when it meets air oxygen during drying and handling, rather than representing an unreacted precursor, the existence of Ag (I) is typical and anticipated in highly reactive, high-surface-area silver nanoparticles. Importantly, the fact that the Ag (0) signal predominates proves that the *A. vacillans* extract has excellent reducing capabilities and guarantees that the nanoparticles have a metal core that causes them to be so effective against bacteria. *A. vacillans,* a botanical marvel, presents a fascinating chemical composition that mirrors the skeletal framework of most plants. Its molecular structure is a harmonious blend of functional groups, including the ubiquitous carboxyl and amino



(a) (b)

Figure 9: SEM images of green-synthesized AgNPs: (a) surface morphology showing particle aggregation. (b) Magnified view highlighting distribution of silver nanoparticles.



(a) (b)

Figure 10: (a) XPS spectra of Ag 3 d for AgNPs; (b) the whole XPS spectrum of AgNPs.

groups. These elements and a diverse array of others paint a vivid picture of the plant's intricate chemistry. As revealed by the XPS survey spectrum, elements such as oxygen, nitrogen, silver, and carbon can seamlessly integrate into its structure, further underscoring its adaptability and potential for various applications. This botanical symphony of chemical components contributes to the unique properties and potential benefits of *A. vacillans*, making it a subject of ongoing scientific exploration, as shown in Figure 10(b).

3.7. Antibacterial Activities of AgNPs. The antibacterial activity of the green-synthesized AgNPs by *A. vacillans* leaves the extract at optimal conditions, and the antibiotic gentamycin against two types of Gram-negative bacteria (*E. coli* and *S. typhi*) and two types of Gram-positive bacteria (*S. aureus* and *B. subtilis*) effects are shown in Figure 11. The AgNPs synthesized by AVL extract inhibition zones against different bacterial strains ranged from 10 mm to 18 mm compared with gentamycin antibiotic [55] (Figure 12). The inhibition zones are listed in Table 5 for the 4 different bacterial strains, which indicate different effects by variation in AgNPs concentration. The higher inhibition zones were observed on Gram-negative bacteria "*S. typhi*" with a good agreement for previous research [34, 38, 59]. It is noteworthy that previous studies have already reported the antibacterial activity of *A. vacillans* extracts alone against Gram-positive and Gram-negative bacteria, including *E. coli* and *Pseudomonas aeruginosa* [60]. Therefore, the antibacterial activity observed in our work can be attributed primarily to the biosynthesized silver nanoparticles rather than solely to the phytochemicals present in the extract.

3.8. Antioxidant Activities of AgNPs. The antioxidant potential of the synthesized AgNPs was investigated using the DPPH free radical assay, a widely recognized method for assessing antioxidant activity. AgNPs synthesized by AVL extract exhibited remarkable scavenging activity, as shown in Figure 13. The percentage of scavenging of silver nanoparticles is calculated in the following equation.

$$\text{DPPH scavenging (\%)} = \left(\frac{A_c - A_S}{Ac}\right) \times 100, \tag{9}$$

where A_c is the absorbance of the control and A_s is the absorbance of the sample.

AgNPs exhibited noticeable scavenging activity at various concentrations (1500, 1000, 500, 250, and 125 µg/mL), ranging from 12.26% to 48.06%. These promising results of Ag nanoparticles are consistent with previous research representing the considerable antioxidant properties [1, 48, 61].

In support of the antioxidant activity of the biosynthesized AgNPs, several studies have reported comparable findings using *Aloe* species. Ghatage et al. demonstrated moderate antioxidant capacity for AgNPs synthesized using *Aloe barbadensis* leaves, while Varadharajan and Pandian [62] reported a free radical scavenging efficiency of up to 75% using *Aloe* root extract [62, 63]. Likewise, Mahboob confirmed that silver

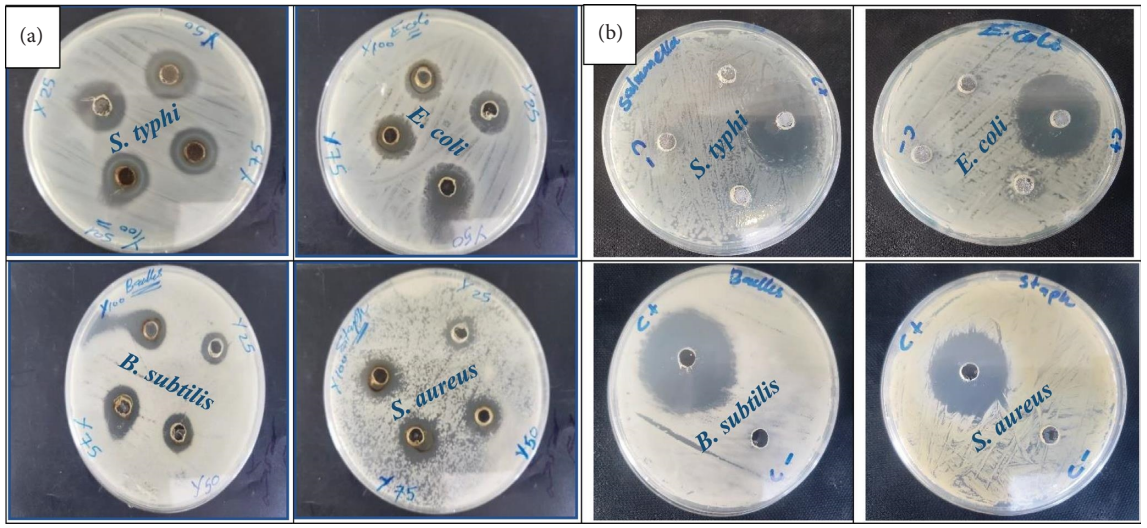


Figure 11: Antibacterial activity of (a) AgNPs and (b) gentamycin against different types of bacteria.

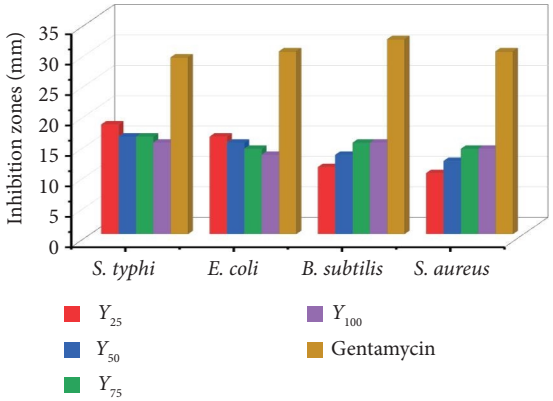


Figure 12: The inhibition zones of gentamycin and the green-synthesized AgNPs in different concentrations.

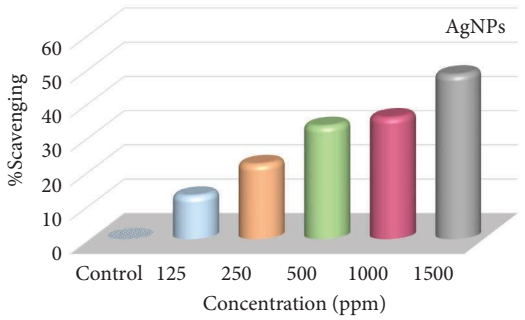


Figure 13: DPPH free radical scavenging activity of the green-synthesized nanoparticles.

Table 5: Results of AgNP antibacterial activities with different bacteria types.

Bacteria type	Bacteria names	Inhibition zones (mm)				
		Y_{25}	Y_{50}	Y_{75}	Y_{100}	Gentamycin
Gram (−) bacteria	*S. typhi*	18	16	16	15	29
	E. coli	16	15	14	13	30
Gram (+) bacteria	*B. subtilis*	11	13	15	15	32
	S. aureus	10	12	14	14	30

nanoparticles synthesized with *Aloe vera* aqueous extract possess considerable antioxidant activity both in *vitro* and in *vivo* [64]. These reports reinforce the observed antioxidant potential in the current study, highlighting the valuable role of phytochemicals from *Aloe* in enhancing AgNPs bioactivity.

4. Conclusion

This study reports the successful synthesis of silver nanoparticles (AgNPs) using *A. vacillans* extract through an environmentally friendly method. Various techniques, including UV-Vis, FTIR, XRD, SEM, EDX, and XPS, confirmed the formation, structure, and composition of the AgNPs. The findings showed that both metallic silver and silver oxide were present, which influenced the nanoparticles' properties. The AgNPs showed moderate antioxidant activity in the DPPH assay and strong antibacterial effects against both Gram-positive and Gram-negative bacteria, suggesting possible uses in medicine and

environmental fields. However, the study did not include MIC/MBC measurements or high-resolution TEM analysis, which is planned for future research. These results suggest that *A. vacillans* can be used to sustainably produce AgNPs, though further work is needed to improve their performance and explore more applications.

Data Availability Statement

The data that support the findings of this study are available from the corresponding author upon reasonable request.

Conflicts of Interest

The authors declare no conflicts of interest.

Author Contributions

Conceptualization: Yasmin M. S. Jamil, Ahmed N. Al-Hakimi, and Ghadeer Y. Al-Mahwiti; methodology: Yasmin M. S. Jamil, Hussein M. A. Al-Maydama, Ahmed N. Al-Hakimi, and Ghadeer Y. Al-Mahwiti; validation: Yasmin M. S. Jamil, Hussein M. A. Al-Maydama, Sayed M. Saleh, and Ghadeer Y. Al-Mahwiti; formal analysis: Hussein M. A. Al-Maydama, Ahmed N. Al-Hakimi, and Ghadeer Y. Al-Mahwiti; investigation: Yasmin M. S. Jamil, Hussein M. A. Al-Maydama, Sayed M. Saleh, Ghadeer Y. Al-Mahwiti, and Basem Al-Akhali; resources: Hassan M. Ibrahim, Yasmin M. S. Jamil, Hussein M. A. Al-Maydama, Ahmed N. Al-Hakimi, and Ghadeer Y. Al-Mahwiti; data curation: Yasmin M. S. Jamil, Hussein M. A. Al-Maydama, Sayed M. Saleh, and Ghadeer Y. Al-Mahwiti; writing–original draft preparation: Yasmin M. S. Jamil and Ghadeer Y. Al-Mahwiti; writing–review and editing: all authors; visualization: Hassan M. Ibrahim, Hussein M. A. Al-Maydama, Ahmed N. Al-Hakimi, and Ghadeer Y. Al-Mahwiti; supervision: Ahmed N. Al-Hakimi, Yasmin M. S. Jamil, and Hussein M. A. Al-Maydama; project administration: Yasmin M. S. Jamil and Hussein M. A. Al-Maydama.

Funding

This study has no funding.

References

[1] Y. M. S. Jamil, A. N. Al-Hakimi, H. M. A. Al-Maydama, G. Y. Almahwiti, A. Qasem, and S. M. Saleh, "Optimum Green Synthesis, Characterization, and Antibacterial Activity of Silver Nanoparticles Prepared From an Extract of *Aloe fleurentinorum*," *International Journal of Chemical Engineering* 2024, no. 1 (2024): 2804165, https://doi.org/10.1155/2024/2804165.

[2] S. M. Saleh, M. K. Almotiri, and R. Ali, "Green Synthesis of Highly Luminescent Gold Nanoclusters and Their Application in Sensing Cu (II) and Hg (II)," *Journal of Photochemistry and Photobiology A: Chemistry* 426 (2022): 113719, https://doi.org/10.1016/j.jphotochem.2021.113719.

[3] R. Ali, B. Alfeneekh, S. Chigurupati, and S. M. Saleh, "Green Synthesis of Pregabalin-Stabilized Gold Nanoclusters and Their Applications in Sensing and Drug Release," *Archiv der Pharmazie* 355, no. 4 (2022): 2100426, https://doi.org/10.1002/ardp.202100426.

[4] S. M. Saleh, F. M. Alminderej, R. Ali, and O. I. Abdallah, "Optical Sensor Film for Metribuzin Pesticide Detection," *Spectrochimica Acta Part A: Molecular and Biomolecular Spectroscopy* 229 (2020): 117971, https://doi.org/10.1016/j.saa.2019.117971.

[5] V. Gupta, S. Mohapatra, H. Mishra, et al., "Nanotechnology in Cosmetics and Cosmeceuticals-A Review of Latest Advancements," *Gels* 8, no. 3 (2022): 173, https://doi.org/10.3390/gels8030173.

[6] A. G. Ponce, J. F. Ayala-Zavala, N. E. Marcovich, F. J. Vázquez, and M. R. Ansorena, "Nanotechnology Trends in the Food Industry: Recent Developments, Risks, and Regulation," *Impact of Nanoscience in the Food Industry* (2018): 113–141, https://doi.org/10.1016/b978-0-12-811441-4.00005-4.

[7] S. M. Saleh, R. Ali, M. E. F. Hegazy, F. M. Alminderej, and T. A. Mohamed, "The Natural Compound Chrysosplenol-D is a Novel, Ultrasensitive Optical Sensor for Detection of Cu (II)," *Journal of Molecular Liquids* 302 (2020): 112558, https://doi.org/10.1016/j.molliq.2020.112558.

[8] S. M. Saleh, W. A. El-Sayed, M. A. El-Manawaty, M. Gassoumi, and R. Ali, "An Eco-Friendly Synthetic Approach for Copper Nanoclusters and Their Potential in Lead Ions Sensing and Biological Applications," *Biosensors* 12, no. 4 (2022): 197, https://doi.org/10.3390/bios12040197.

[9] S. M. Saleh, "ZnO Nanospheres Based Simple Hydrothermal Route for Photocatalytic Degradation of Azo Dye," *Spectrochimica Acta Part A: Molecular and Biomolecular Spectroscopy* 211 (2019): 141–147, https://doi.org/10.1016/j.saa.2018.11.065.

[10] A. E. A. E. Albadri, M. A. B. Aissa, A. Modwi, and S. M. Saleh, "Synthesis of Mesoporous ru-ZnO@g-C3N4 Nanoparticles and Their Photocatalytic Activity for Methylene Blue Degradation," *Water* 15, no. 3 (2023): 481, https://doi.org/10.3390/w15030481.

[11] S. M. Saleh, A. E. A. E. Albadri, M. A. B. Aissa, and A. Modwi, "Fabrication of Mesoporous V2O5@g-C3N4 Nanocomposite as Photocatalyst for Dye Degradation," *Crystals* 12 (2022): 1766, https://doi.org/10.3390/cryst12121766.

[12] A. H. Al Hammadi, A. Al Sharabi, and A. Alnehia, "Green and Chemically Prepared Zinc Sulfide Nanoparticles: A Comparative Study," *Sana'a University Journal of Applied Sciences and Technology* 1 (2023): 70–77, https://doi.org/10.59628/jast.v1i1.104.

[13] W. Abdussalam-Mohammed, "Comparison of Chemical and Biological Properties of Metal Nanoparticles (Au, Ag), With Metal Oxide Nanoparticles (ZnO-NPs) and Their Applications," *Advanced Journal of Chemistry, Section A* 3 (2020): 192–210, https://doi.org/10.33945/SAMI/AJCA.2020.2.8.

[14] H. M. Fahmy, A. M. Mosleh, A. A. Elghany, et al., "Coated Silver Nanoparticles: Synthesis, Cytotoxicity, and Optical Properties," *RSC Advances* 9, no. 35 (2019): 20118–20136, https://doi.org/10.1039/C9RA02907A.

[15] K. P. Steckiewicz, P. Cieciórski, E. Barcińska, et al., "Silver Nanoparticles as Chlorhexidine and Metronidazole Drug Delivery Platforms: Their Potential Use in Treating Periodontitis," *International Journal of Nanomedicine* 17 (2022): 495–517, https://doi.org/10.2147/IJN.S339046.

[16] J. M. Domingues, C. S. Miranda, N. C. Homem, H. P. Felgueiras, and J. C. Antunes, "Nanoparticle Synthesis and Their Integration Into Polymer-Based Fibers for

Biomedical Applications," *Biomedicines* 11, no. 7 (2023): 1862, https://doi.org/10.3390/biomedicines11071862.

[17] S. N. Nandhini, N. Sisubalan, A. Vijayan, et al., "Recent Advances in Green-Synthesized Nanoparticles for Bactericidal and Wound Healing Applications," *Heliyon* 9, no. 2 (2023): 13128, https://doi.org/10.1016/j.heliyon.2023.e13128.

[18] P. Dikshit, J. Kumar, A. Das, et al., "Green Synthesis of Metallic Nanoparticles: Applications and Limitations," *Catalysts* 11, no. 8 (2021): 902, https://doi.org/10.3390/catal11080902.

[19] A. Singh, B. Madhavi, and M. N. Nithin Sagar, "An Overview of Green Synthesis Mediated Metal Nanoparticles Preparation and Its Scale up Opportunities," *Journal of Drug Delivery and Therapeutics* 11, no. 6 (2021): 304–314, https://doi.org/10.22270/jddt.v11i6.5082.

[20] A. Zuhrotun, D. J. Oktaviani, and A. N. Hasanah, "Biosynthesis of Gold and Silver Nanoparticles Using Phytochemical Compounds," *Molecules* 28, no. 7 (2023): 3240, https://doi.org/10.3390/molecules28073240.

[21] M. Patel, R. R. Singh, and S. K. Singh, "Green Synthesis of Silver Nanoparticles: Methods, Biological Applications, Delivery and Toxicity," *Materials Advances* 4 (2023): 1831–1849, https://doi.org/10.1039/d2ma01105k.

[22] C. Buzea, I. I. Pacheco, K. Robbie, et al., "Nanomaterials and Nanoparticles: Sources and Toxicity," *Biointerphases* 2, no. 4 (2007): MR17–MR71, https://doi.org/10.1116/1.2815690.

[23] A. Malakar, S. R. Kanel, C. Ray, et al., "Nanomaterials in the Environment, Human Exposure Pathway, and Health Effects: A Review," *The Science of the Total Environment* 759 (2021): 143470, https://doi.org/10.1016/j.scitotenv.2020.143470.

[24] U. Kamran, H. N. Bhatti, M. Iqbal, and A. Nazir, "Green Synthesis of Metal Nanoparticles and Their Applications in Different Fields: A Review," *Zeitschrift für Physikalische Chemie* 233, no. 9 (2019): 1325–1349, https://doi.org/10.1515/zpch-2018-1238.

[25] A. Wasilewska, U. Klekotka, M. Zambrzycka, G. Zambrowski, I. Święcicka, and B. Kalska-Szostko, "Physico-Chemical Properties and Antimicrobial Activity of Silver Nanoparticles Fabricated by Green Synthesis," *Food Chemistry* 400 (2023): 133960–133967, https://doi.org/10.1016/j.foodchem.2022.133960.

[26] P. Tippayawat, N. Phromviyo, P. Boueroy, and A. Chompoosor, "Green Synthesis of Silver Nanoparticles in *Aloe vera* Plant Extract Prepared by a Hydrothermal Method and Their Synergistic Antibacterial Activity," *PeerJ* 4 (2016): e2589, https://doi.org/10.7717/peerj.2589.

[27] L. Castillo-Henríquez, K. Alfaro-Aguilar, J. Ugalde-Álvarez, G. Montes de Oca-Vásquez, and J. Roberto Vega-Baudrit, "Green Synthesis of Metal Nanoparticles From Plant Extracts, and Their Possible Application as Antimicrobial Agents in the Agricultural Area," *Preprints* (2020): https://doi.org/10.20944/preprints202007.0318.v1.

[28] E. R. Carmona, N. Benito, T. Plaza, and G. Recio-Sánchez, "Green Synthesis of Silver Nanoparticles by Using Leaf Extracts From the Endemic Buddleja Globosa Hope," *Green Chemistry Letters and Reviews* 10, no. 4 (2017): 250–256, https://doi.org/10.1080/17518253.2017.1360400.

[29] M. S. Rafique, I. Sadaf, M. S. Rafique, and M. B. Tahir, "A Review on Green Synthesis of Silver Nanoparticles and Their Applications," *Artificial Cells, Nanomedicine, and Biotechnology* 45 (2016): 1–20, https://doi.org/10.1080/21691401.2016.1241792.

[30] A. K. Mittal, Y. Chisti, and U. C. Banerjee, "Synthesis of Metallic Nanoparticles Using Plant Extracts," *Biotechnology Advances* 31, no. 2 (2013): 346–356, https://doi.org/10.1016/j.biotechadv.2013.01.003.

[31] M. F. Baran, C. Keskin, A. Baran, et al., "Green Synthesis of Silver Nanoparticles From *Allium cepa L*. Peel Extract, Their Antioxidant, Antipathogenic, and Anticholinesterase Activity," *Molecules* 28, no. 5 (2023): 2310–2317, https://doi.org/10.3390/molecules28052310.

[32] K. Sharma, S. Guleria, K. H. Salaria, et al., "Photocatalytic and Biological Properties of Silver Nanoparticles Synthesized Using *Callistemon lanceolatus* Leaf Extract," *Industrial Crops and Products* 202 (2023): 116951–17, https://doi.org/10.1016/j.indcrop.2023.116951.

[33] K. D. Dejen, D. Y. Kibret, T. H. Mengesha, et al., "Green Synthesis and Characterisation of Silver Nanoparticles From Leaf and Bark Extract of *Croton macrostachyus* for Antibacterial Activity," *Materials Technology* 38 (2023): 2164647–10, https://doi.org/10.1080/10667857.2022.2164647.

[34] A. N. Al-Hakimi, T. M. Alresheedi, and R. A. Albarrak, "The Effect of the Saudi *Haloxylon ammodendron Shrub* on Silver Sanoparticles: Optimal Biosynthesis, Characterization, Removability of Mercury Ions, Antimicrobial and Anticancer Activities," *Inorga* 11 (2023): 1–16, https://doi.org/10.3390/inorganics11060246.

[35] M. Naveed, B. Bukhari, T. Aziz, et al., "Green Synthesis of Silver Nanoparticles Using the Plant Extract of *Acer oblongifolium* and Study of its Antibacterial and Antiproliferative Activity via Mathematical Approaches," *Molecules* 27, no. 13 (2022): 4226, https://doi.org/10.3390/molecules27134226.

[36] P. Singh and I. Mijakovic, "Green Synthesis and Antibacterial Applications of Gold and Silver Nanoparticles From *Ligustrum vulgare* Berries," *Scientific Reports* 12 (2022): 7902–7912, https://doi.org/10.1038/s41598-022-11811-7.

[37] C. M. Vieyra, M. T. Olguin, E. G. Segura, and G. L. Tellez, "Comparison of Ag, Cu and Zn Nanoparticles Obtained Using *Aloe vera* Extract and Gamma Ionizing Radiation," *Journal of Applied Research and Technology* 18, no. 5 (2020): 289–314, https://doi.org/10.22201/icat.24486736e.2020.18.5.1284.

[38] M. Yadav, J. P. Kumar, S. Budhwar, L. Yadav, and A. and Yadav, "Characterization and Antibacterial Activity of Synthesized Silver and Iron Nanoparticles Using *Aloe vera*," *Journal of Nanomedicine & Nanotechnology* 7, no. 3 (2016): 1–7, https://doi.org/10.4172/2157-7439.1000384.

[39] G. Supriya and S. Chaitanya Kumari, "Green Synthesis of Silver Nanoparticles Using *Aloe vera* Extract and Assessing Their Antimicrobial Activity Against Skin Infections," *International Journal of Scientific Research in Biological Sciences* 6 (2019): 60–65, https://doi.org/10.26438/ijsrbs/v6si1.6065.

[40] T. R. Anju, S. Parvathy, M. Valiya Veettil, et al., "Green Synthesis of Silver Nanoparticles From *Aloe vera* Leaf Extract and Its Antimicrobial Activity," *Materials Today: Proceedings* 43 (2021): 3956–3960, https://doi.org/10.1016/j.matpr.2021.02.665.

[41] A. Rautela, J. Rani, and M. Debnath (Das), "Green Synthesis of Silver Nanoparticles From *Tectona grandis* Seeds Extract: Characterization and Mechanism of Antimicrobial Action on Different Microorganisms," *Journal of Analytical Science and Technology* 10 (2019): 1–10, https://doi.org/10.1186/s40543-018-0163-z.

[42] P. B. E. Kedi, F. E. Meva, L. Kotsedi, et al., "Eco-Friendly Synthesis, Characterization, in *Vitro* and in *Vivo* Anti-Inflammatory Activity of Silver Nanoparticle-Mediated *Selaginella myosurus* Aqueous Extract," *International Journal of Nanomedicine* 13 (2018): 8537–8548, https://doi.org/10.2147/IJN.S174530.

[43] D. K. Adeyemi, A. O. Adeluola, M. J. Akinbile, O. O. Johnson, and G. A. Ayoola, "Green Synthesis of Ag, Zn and Cu Nanoparticles From Aqueous Extract of *Spondias mombin* Leaves and Evaluation of Their Antibacterial Activity," *African Journal of Clinical and Experimental Microbiology* 21, no. 2 (2020): 106–113, https://doi.org/10.4314/ajcem.v21i2.4.

[44] A. A. Kajani, A. K. Bordbar, S. H. Zarkesh Esfahani, A. R. Khosropour, and A. Razmjou, "Green Synthesis of Anisotropic Silver Nanoparticles With Potent Anticancer Activity Using *Taxus baccata* Extract," *RSC Advances* 4, no. 106 (2014): 61394–61403, https://doi.org/10.1039/c4ra08758e.

[45] K. Shameli, M. Ahmad, A. Zamanian, et al., "Green Biosynthesis of Silver Nanoparticles Using *Curcuma longa* Tuber Powder," *International Journal of Nanomedicine* 7 (2012): 5603–5610, https://doi.org/10.2147/IJN.S36786.

[46] S. Jain and M. S. Mehata, "Medicinal Plant Leaf Extract and Pure Flavonoid Mediated Green Synthesis of Silver Nanoparticles and Their Enhanced Antibacterial Property," *Scientific Reports* 7 (2017): 15867, https://doi.org/10.1038/s41598-017-15724-8.

[47] G. Rehman, M. Umar, N. Shah, et al., "Green Synthesis and Characterization of Silver Nanoparticles Using *Azadirachta indica* Seeds Extract: in *Vitro* and in *Vivo* Evaluation of Anti-Diabetic Activity," *Pharmaceuticals* 16, no. 12 (2023): 1677, https://doi.org/10.3390/ph16121677.

[48] S. Jaw, A. Arthanari, and S. Rajeshk, "Antioxidant Activity of Silver Nanoparticles Synthesized Using *Vetiveria zizanioides*-in *Vitro* Study," *Journal of Research in Medical and Dental Science* 9 (2021): 199–203.

[49] E. K. Kocazorbaz, "Green Synthesis, Optimization, and Characterization of Silver Nanoparticles From *Euphorbia rigida* Leaf Extract and Investigation of Their Antimicrobal Activities," *Bilecik Seyh Edebali University Journal of Science* 8 (2021): 512–522, https://doi.org/10.35193/bseufbd.843005.

[50] M. Sharifi-rad, H. S. Elshafie, and P. Pohl, "Green Synthesis of Silver Nanoparticles (AgNPs) by *Lallemantia royleana* Leaf Extract: Their Bio-Pharmaceutical and Catalytic Properties," *Journal of Photochemistry and Photobiology A: Chemistry* 448 (2024): 115318, https://doi.org/10.1016/j.jphotochem.2023.115318.

[51] H. M. Ibrahim, A. R. Alshaibani, and A. N. A. Al-Gifri, "Epidermal Properties of *Aloe vacillans Forsskål* Leaf and Its Taxonomical Significance in Classifying Its Two Forms," *PSM Biological Research* 6 (2021): 76–83.

[52] A. K. Hegazy and J. Lovett-Doust, *Plant Ecology in the Middle East* (Oxford University Press, 2016).

[53] Y. M. S. Jamil, F. M. Al-azab, N. A. A. Al-selwi, A. M. AL-Ryami, and M. R. Mlahia, "Spectroscopic and Biological Studies of Mixed Ligand Complexes of Transition Metal (II) Ions with Chloroquine and Ketoprofen," *Sana'a University Journal of Applied Sciences and Technology* 2, no. 1 (2024): 53–64, https://doi.org/10.59628/jast.v2i1.801.

[54] Y. M. S. Jamil, M. A. H. Awad, and H. M. A. Al-maydama, "Physicochemical Properties and Antibacterial Activity of Pt Nanoparticles on TiO_2 Nanotubes as Electrocatalyst for Methanol Oxidation Reaction," *Results in Chemistry* 4 (2022): 100531, https://doi.org/10.1016/j.rechem.2022.100531.

[55] Y. M. S. Jamil, H. M. A. Al-Maydama, A. N. Al-Hakimi, G. Y. S. Al-Mahwiti, H. M. Ibrahim, and B. Al-Akhali, "Characterization, Antibacterial and Antioxidant of Phyto-synthesized Zinc Oxide Nanoparticles Using *Aloe fleurentinorum* Leaves Extract," *Sana'a University Journal of Applied Sciences and Technology* 2, no. 4 (2024): 339–347, https://doi.org/10.59628/jast.v2i4.1011.

[56] S. Bhakya, S. Muthukrishnan, M. Sukumaran, and M. Muthukumar, "Biogenic Synthesis of Silver Nanoparticles and Their Antioxidant and Antibacterial Activity," *Applied Nanoscience* 6, no. 5 (2016): 755–766, https://doi.org/10.1007/s13204-015-0473-z.

[57] Y. M. S. Jamil, M. A. H. Awad, H. M. A. Al-Maydama, et al., "Gold Nanoparticles Loaded on TiO_2 Nanoparticles Doped With N_2 as an Efficient Electrocatalyst for Glucose Oxidation: Preparation, Characterization, and Electrocatalytic Properties," *Journal of Analytical Science and Technology* 13, no. 1 (2022): 54, https://doi.org/10.1186/s40543-022-00363-0.

[58] Y. M. S. Jamil, M. A. H. Awad, H. M. A. Al-Maydama, Y. EL-Ghoul, and A. N. Al-Hakimi, "Synthesis and Study of Enhanced Electrochemical Properties of Nio Nanoparticles Deposited on TiO_2 Nanotubes," *Applied Organometallic Chemistry* 36 (2022): 1–15, https://doi.org/10.1002/aoc.6795.

[59] A. Khan, A. Shaheen, and W. Rehman, "Yaqoob, Novel Synthesis and Characterization of Silver Nanoparticles From Leaf Aqueous Extract of *Aloe vera* and Their Anti-Microbial Activity," *Journal of Nanoscience, Nanoengineering & Applications* 1 (2017): 1–9.

[60] A. A. F. Khardesh, H. Q. M. Hadi, and K. S. Ali, "Antibacterial Activity of *Aloe lanata* and *Aloe Vacillanis* Plant Extracts, Electron," *Electronic Journal of University of Aden for Basic and Applied Sciences* 1 (2020): 20–24, https://doi.org/10.47372/ejua-ba.2020.1.6.

[61] A. Arya, P. K. Tyagi, S. Bhatnagar, R. K. Bachheti, A. Bachheti, and M. Ghorbanpour, "Biosynthesis and Assessment of Antibacterial and Antioxidant Activities of Silver Nanoparticles Utilizing *Cassia occidentalis L.* Seed," *Scientific Reports* 14 (2024): 7243, https://doi.org/10.1038/s41598-024-57823-3.

[62] S. Varadharajan and P. Pandian, "Antioxidant, Antimicrobial, and Potential Biomedical Applications of Green Synthesized Silver Nanoparticles Using *Aloe barbadensis* Root," *Journal of Environmental Nanotechnology* 14, no. 1 (2025): 97–104, https://doi.org/10.13074/jent.2025.03.2511226.

[63] M. M. Ghatage, P. A. Mane, R. P. Gambhir, et al., "Green Synthesis of Silver Nanoparticles via *Aloe barbadensis Miller* Leaves: Anticancer, Antioxidative, Antimicrobial and Photocatalytic Properties," *Applied Surface Science Advances* 16 (2023): 100426, https://doi.org/10.1016/j.apsadv.2023.100426.

[64] T. Mahboob, "Evaluation of Antioxidant Activity of Biologically Synthesized Silver Nanoparticles Using *Aloe vera*," *International Journal of Biology and Biotechnology* 16 (2019): 641–653.